



In silico promoter analysis and functional validation identify CmZFH, the co-regulator of hypoxia-responsive genes *CmScylla* and *CmLPCAT*

Li He^{a,b,c}, Ivy W. Chen^{b,c}, Zan Zhang^d, Wenping Zheng^e, Ahmed Sayadi^f, Lei Wang^{b,c,1}, Wen Sang^{b,c,2}, Rui Ji^{b,c,3}, Jiaxin Lei^{b,c}, Göran Arnqvist^f, Chaoliang Lei^a, Keyan Zhu-Salzman^{b,c,*}

^a Hubei Insect Resources Utilization and Sustainable Pest Management Key Laboratory, College of Plant Science and Technology, Huazhong Agricultural University, Wuhan, 430070, China

^b Department of Entomology, Texas A&M University, College Station, TX, 77843, USA

^c Institute for Plant Genomics & Biotechnology, Texas A&M University, College Station, TX, 77843, USA

^d Key Laboratory of Entomology and Pest Control Engineering, College of Plant Protection, Academy of Agricultural Sciences, Southwest University, Chongqing, 400716, China

^e Key Laboratory of Horticultural Plant Biology (MOE), Institute of Urban and Horticultural Entomology, College of Plant Science and Technology, Huazhong Agricultural University, Wuhan, 430070, China

^f Animal Ecology, Department of Ecology and Genetics, Uppsala University, Uppsala, 75236, Sweden

ARTICLE INFO

Keywords:

Callosobruchus maculatus

Hypoxia

Common *cis*-element

AREB6

CmZFH

Zinc-finger cluster

ABSTRACT

Oxygen (O₂) plays an essential role in aerobic organisms including terrestrial insects. Under hypoxic stress, the cowpea bruchid (*Callosobruchus maculatus*) ceases feeding and growth. However, larvae, particularly 4th instar larvae exhibit very high tolerance to hypoxia and can recover normal growth once brought to normoxia. To better understand the molecular mechanism that enables insects to cope with low O₂ stress, we performed RNA-seq to distinguish hypoxia-responsive genes in midguts and subsequently identified potential common *cis*-elements in promoters of hypoxia-induced and -repressed genes, respectively. Selected elements were subjected to gel-shift and transient transfection assays to confirm their *cis*-regulatory function. Of these putative common *cis*-elements, *AREB6* appeared to regulate the expression of *CmLPCAT* and *CmScylla*, two hypoxia-induced genes. CmZFH, the putative *AREB6*-binding protein, was hypoxia-inducible. Transient expression of CmZFH in *Drosophila* S2 cells activated *CmLPCAT* and *CmScylla*, and their induction was likely through interaction of CmZFH with *AREB6*. Binding to *AREB6* was further confirmed by bacterially expressed CmZFH recombinant protein. Deletion analyses indicated that the N-terminal zinc-finger cluster of CmZFH was the key *AREB6*-binding domain. Through *in silico* and experimental exploration, we discovered novel transcriptional regulatory components associated with gene expression dynamics under hypoxia that facilitated insect survival.

1. Introduction

Hypoxia, or O₂ deprivation, is a state in which the O₂ demand of an organism exceeds what is available. As a result, biological functions of aerobic organisms including terrestrial insects are adversely affected, leading to retarded growth and development and even death of the organisms (Harrison et al., 2018). Many insect species including

coleopterans, dipterans, lepidopterans, isopteran, hymenopteran and orthopteran, particularly those living in hypoxic habitats, have developed certain levels of tolerance to hypoxia and many can recover from hours to weeks of exposure to hypoxia and anoxia (Hoback and Stanley, 2001). For example, red flour beetle (*Tribolium castaneum*) adults can tolerate 2% O₂ for more than 10 days (Kharel et al., 2019). *Drosophila melanogaster* can survive in a constant 4% O₂ environment (Zhou et al., 2008). High-altitude locusts (*Locusta migratoria*) are more tolerant to

* Corresponding author. Department of Entomology, Texas A&M University, College Station, TX, 77843, USA.

E-mail address: ksalzman@tamu.edu (K. Zhu-Salzman).

¹ School of Grain Science and Technology, Jiangsu University of Science and Technology, Zhenjiang 212100, China.

² Department of Entomology, South China Agricultural University, Guangzhou 510640, China.

³ Institute of Plant Protection, Jiangsu Academy of Agricultural Sciences, Jiangsu Key Laboratory for Food and Safety-State Key Laboratory Cultivation Base of Ministry of Science and Technology, Nanjing 210014, China.

Abbreviations

ZFH	Zinc-finger homeodomain
LPCAT	Lysophosphatidylcholine acyltransferase
HIF1	Hypoxia-inducible factor 1
RT-qPCR	Reverse transcription-quantitative PCR
EMSA	Electrophoretic mobility shift assay
LUC	Luciferase
GO	Gene ontology
KEGG	Kyoto encyclopedia of genes and genomes
NE	Nuclear extract
FPKM	Fragments per kilobase of exon per million mapped fragments
IPTG	Isopropyl- β -D-thiogalactopyranoside

extreme hypoxia than low-altitude locusts (Zhao et al., 2013). Hypoxia even enhances survival of overwintering *Megachile rotundata* prepupae (Abdelrahman et al., 2014) and reproduction in the subterranean termite royals (*Reticulitermes speratus*) (Tasaki et al., 2018).

Some progress has been made in understanding how insects cope with a limited O₂ supply. Strategies like changing behavior or adjusting metabolic processes are often employed by hypoxic insects. Both larvae and adults of *Drosophila* reduce food intake and alter feeding behavior and/or diet preference to cope with low O₂ (Farzin et al., 2014; Vigne and Frelin, 2010; Wingrove and O'Farrell, 1999). To aid O₂ uptake, caddisfly (*Hydropsyche angustipennis*) larvae increase their ventilation rate under hypoxia (Van der Geest, 2007). *Drosophila* even increases the diameter of tracheoles and the number of tracheal branches to enhance O₂ delivery to internal tissues (VandenBrooks et al., 2018). By lowering O₂ pressure from 3 to 0.5 kPa, *Drosophila* exhibited a rapid and linear reduction of approximately 10-fold in its metabolic rate (Van Voorhies, 2009). Reducing energy demand helps insects tolerate lack of O₂: hypoxia inhibits protein translation in *Drosophila* S2 cells (Lee et al., 2008), one of the most energy-consuming process (Buttgereit and Brand, 1995). The nitric oxide pathway is known to contribute to *Drosophila*'s ability to respond to O₂ deprivation by arresting cell cycles in embryo and larvae, as well as protecting cells from hypoxia-induced injury (Mahneva et al., 2019; Wingrove and O'Farrell, 1999).

It is well known that insects alter expression of a large number of genes to cope with low O₂ stress (Li et al., 2013; Zhao et al., 2012). A common mechanism that controls transcript abundance is through nuclear factor(s) binding to cognate promoter *cis*-element(s), causing induction or suppression of the gene(s). Of the known transcription factors regulating hypoxia-responsive genes, the best studied is the ubiquitous hypoxia-inducible factor 1 (HIF1) (Gorr et al., 2006). In insects, this transcriptional regulator has been reported to activate O₂-dependent transcription of a large number of genes, including those participating in growth inhibition and tracheal terminal sprouting (Centanin et al., 2008; Reiling and Hafen, 2004), leading to increased low O₂ endurance. The presence of common binding elements in genes encoding TCA cycle or β -oxidation enzymes (but absence in others) led to the discovery of the transcription factor, hairy. This metabolic switch is responsible for down-regulating these genes in hypoxia-tolerant *Drosophila*. Mutation of hairy abolishes such suppression (Zhou et al., 2008). In addition, mutation in the transcription factor *forkhead box O* (*FOXO*) blocks the hypoxia-induced increase in mRNA of *Relish* and its target genes, resulting in a decreased survival in both *Drosophila* adults and larvae (Barretto et al., 2020). Hypoxic *L. migratoria* suppresses cytochrome c oxidase subunits most likely through downregulating its regulator, nuclear respiratory factor-2 (*NRF2*) (Ongwijitwat and Wong-Riley, 2005; Zhao et al., 2012).

Analysis of genomic sequences and transcriptomic data has revealed that genes expressed under similar conditions and/or in the same tissues

may share similar motifs in their promoters, the central control of the transcriptional process (Werner et al., 2003). These common *cis*-elements can be bound and co-regulated by a relatively small number of transcription factors in response to a certain stimulus or challenge, e.g. co-suppression via hairy (Zhou et al., 2008). Despite highly variable sequences among common *cis*-elements, software packages such as Common TFs have been designed to recognize transcription factor-binding sites based on the short conserved nucleotide cores. The binding affinity is reflected by the consensus score. Using this approach, Yu et al. (2015) have successfully identified *cis*-elements in sets of co-expressed genes and their cognate transcription co-regulators during maize leaf development.

The cowpea bruchid (*Callosobruchus maculatus*) is a devastating storage pest of cowpeas and other grain legumes (Jackai and Daoust, 1986). By limiting the O₂ availability in storage facilities needed for insect development, hermetic storage has emerged as a viable chemical-free method to control bruchid damage and preserve the grain quality (Silva et al., 2018). Without adequate O₂, delayed growth and decreased survival rate have been observed in cowpea bruchids at all developmental stages. Given that the larvae feed and develop inside the seeds, an environment likely having limited supplies of O₂, it is reasonable to assume that they have evolved an ability to respond to and resist hypoxia. Indeed, some 4th instar larvae can survive up to 20 days of exposure to 2% O₂ and recover normal development once O₂ resumed to the normoxic level (Cheng et al., 2012). Beside CmHIF1-mediated upregulation of genes encoding small heat shock proteins, very little is known about the molecular components involved in transcriptional control of hypoxia-responsive genes in this storage pests. In this study, we attempted to identify novel transcriptional regulatory components in cowpea bruchids through the combination of *in silico cis*-element identification and functional validation experiments. Co-regulation of hypoxia-responsive genes via a zinc-finger homeodomain (ZFH) transcription factor presumably contributed to bruchid tolerance to hypoxic stress.

2. Materials and Methods

2.1. Insect rearing and hypoxia treatment

Cowpea bruchids were maintained on cowpea seeds as previously described (Wang et al., 2019). When larvae reached the 4th instar, infested seeds were transferred into 1 L septum bottles (Industrial glassware, Millville, NJ). The bottles were then filled with pre-mixed gases (2% O₂ + 18% CO₂ + 80% N₂) as described by Cheng et al. (2012) and instantly sealed with parafilm. Levels of O₂ and CO₂ in the bottles were verified with a head-space analyzer (Mocon-PAC CHECK® Model 325, Minneapolis, MN). At the end of the hypoxia treatment (4, 8 or 24 h), gas contents were measured again to ensure airtightness prior to opening of the bottles. To minimize complication caused by tissue specificity, we limited our study to the midgut tissue, the activity of which was highly impacted by availability of environmental O₂. Midguts were instantly dissected in the dissection buffer (100 mM sodium acetate, 1 mM ethylenediaminetetraacetic acid (EDTA), pH 5.5) once larvae were removed from the seeds. Larvae without hypoxia exposure served as the experimental control.

2.2. RNA-seq

Total RNA was extracted from 40 midguts of control or hypoxia-treated 4th instar larvae using TRIzol (Invitrogen, Carlsbad, CA) followed by treatment of RNase-Free DNase I (Qiagen, Valencia, CA) to remove genomic DNA, and purification via RNeasy Mini Kit (Qiagen). Purified RNA was quantified using the NanoDrop ND-1000 spectrophotometer (NanoDrop Technologies, Wilmington, DE) and its integrity was examined with Agilent Bioanalyzer (Agilent Technologies, Palo Alto, CA). TruSeq RNA Sample Preparation Kit (Illumina, San Diego, CA)

was used for mRNA isolation and cDNA library construction. After quality check, transcriptome sequencing were performed on an Illumina HiSeq 2500 platform with 125-nucleotide (nt) paired-end reads at Texas A&M AgriLife Genomics and Bioinformatics Services (College Station, TX). Three biological replicates of treated and control samples were performed, respectively.

2.3. De novo assembly and gene annotation

Raw reads from control or hypoxia-treated samples were cleaned by filtering out adaptor sequences and short or low-quality reads ('N' bases >5% or Phred quality score <10), followed by assembly of filtered reads using Trinity v2.4.0 with default parameters. Unigenes were annotated by BLASTx search (v 2.2.26+) against NCBI non-redundant (Nr) database (E-value <10⁻⁵).

2.4. Identification of hypoxia-responsive genes

Clean reads from each biological replicate were aligned to the assembled transcriptome using Bowtie v1.1.2 (Langmead et al., 2009) and quantified by the eXpress 1.5.1 software (Roberts and Pachter, 2013) to calculate fragments per kilobase of exon per million mapped fragments (FPKM) values. The read counts were input to DESeq2 package (Love et al., 2014) and the differential gene expression was assessed using the negative binomial distribution test. *P*-values were adjusted using the Benjamini-Hochberg adjustment. Unigenes were considered differentially expressed if the adjusted *P*-value i.e. *Q*-value ≤ 0.05 and the absolute log₂ (fold change) value ≥ 1. Blast2GO was applied to obtain the Gene Ontology (GO) annotation of the

hypoxia-responsive genes, and all GO terms were functionally classified using the WEGO software (<http://wego.genomics.org.cn/>) (Ye et al., 2006, 2018). KEGG pathway analysis was conducted using iPathCons in InsectBase (Zhang et al., 2014).

Reverse transcription-quantitative PCR (RT-qPCR) was performed as described in Wang et al. (2019) and *XRCC1* and *XRCC3* served as the negative control (Wang et al., 2019).

2.5. Identification of putative promoters of selected genes and common regulatory cis-elements

Hypoxia-responsive genes with the translation start codon and known functions, i.e. either involved in KEGG pathways or having GO terms, were selected. Assembled mRNAs were aligned with the genomic DNA (European Nucleotide Archive, accession PRJEB30475) (Sayadi et al., 2019), and approximately 1 kb genomic DNA flanking 5' of each transcript was defined as its promoter.

Common TFs and MatInspector (v 8.4.2), two search tools in the Genomatix Software Suite (<http://www.genomatix.de>), were used for promoter analysis. Both software tools utilize a large library of matrix descriptions for transcription factor-binding sites to locate matches in input nucleotide sequences (Cartharius et al., 2005; Quandt et al., 1995). We divided the promoters obtained above into induced and repressed groups, and applied Common TFs to identify *cis*-elements shared by all selected genes of each group in defined promoter regions. The parameters for the common *cis*-element analysis were: 1) the core similarity = 1.0; 2) the matrix similarity = optimized value - 0.02 (Fig. 1). Common *cis*-element consensus logos unique for hypoxia-responsive genes in cowpea bruchids were generated by the WebLogo (<http://weblogo.th>

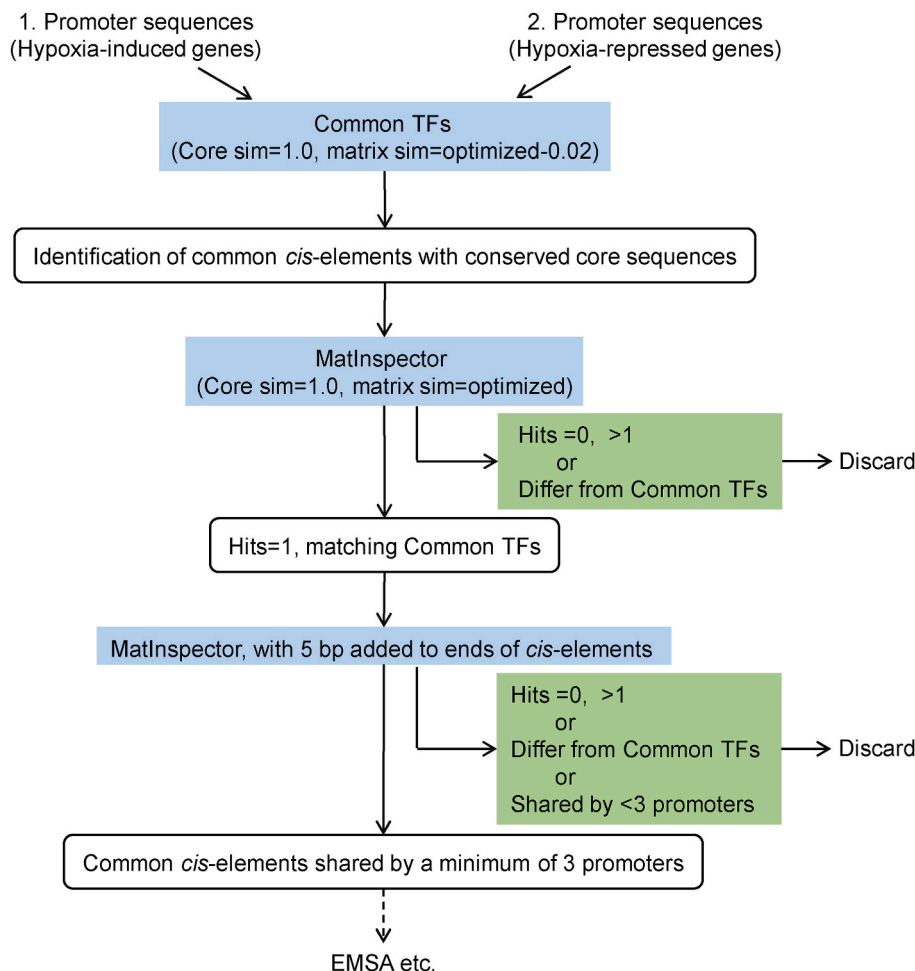


Fig. 1. Flowchart for identification of common regulatory *cis*-elements and selection of candidates for further analysis. Common TFs was applied to analyze promoter sequences of (1) hypoxia-induced and (2) hypoxia-repressed genes to identify respective *cis*-elements commonly shared by all genes in each group. These putative *cis*-elements were then individually confirmed with increased cutoff stringency (shown in boxes shaded blue) or rejected (as indicated in boxes shaded green) by MatInspector for further experimental verification. Addition of 5 bp to both ends of each *cis*-element (to ensure double-stranding in probes) presented more limitation in the candidate *cis*-element selection process streamlined. (For interpretation of the references to color in this figure legend, the reader is referred to the Web version of this article.)

replusone.com/) (Crooks et al., 2004). To acquire optimal number of *cis*-elements potentially involved in co-regulation of hypoxia-responsive gene, we then used MatInspector to select those that had only one *cis*-element hit and this *cis*-element had to match the identity derived from Common TFs. This had to be true even after 5 bp oligos were added to both ends of the *cis*-element. Parameters were: 1) the core similarity = 1.0, and 2) the matrix similarity = the optimized value (Fig. 1). From common *cis*-elements shared by a minimum of 3 promoters after the screening process, we selected a *cis*-element from each of the 3 promoters to perform electrophoretic mobility shift assays (EMSAs) based on their positions in the promoter and the matrix similarity value.

2.6. Nuclear protein extraction and quantification, and EMSA

Nuclear proteins were extracted from freshly dissected midguts of 4th instar larvae using the Nuclear Extract kit (Active Motif, Carlsbad, CA) as we previously described (Ahn et al., 2010). To minimize experimental variation, 5 batches of nuclear extracts from a total of 750 dissected midguts were pooled from hypoxic and normoxic larvae, respectively. Extracts were quantified by the Bradford assay (Bio-Rad) (Bradford, 1976) and confirmed by Western blot analysis. Equal concentrations of hypoxia-treated and normoxic control extracts were stored in -80°C in 10 μL aliquots (1 $\mu\text{g}/\mu\text{L}$) until use.

To radiolabel DNA probes, single-stranded oligonucleotides (Table S2) were end-labeled separately with [γ - ^{32}P] ATP (PerkinElmer, Waltham, MA) using T4 DNA polynucleotide kinase (NEB) as previously described (Ahn et al., 2007). Notably, to ensure the oligos used in the EMSA were double-stranded after annealing, 5 bp of GC-rich oligonucleotides were added to both ends of the selected *cis*-element sequence.

Two μg of nuclear extract was incubated with the radiolabeled probe in binding buffer (4% glycerol, 1 mM MgCl_2 , 0.5 mM EDTA, 0.5 mM dithiothreitol, 0.05 $\mu\text{g}/\mu\text{L}$ of poly (dI-dC), 10 mM Tris-HCl, pH 7.5) for 20 min at room temperature. For competition assays, excess of unlabeled wild-type or mutated competitor was incubated with nuclear extract for 20 min at room temperature prior to the addition of probes. Samples were resolved on the 4% native polyacrylamide gel, followed by X-ray film exposure.

2.7. Construction of reporter plasmids

Genomic DNA was isolated from 5 midguts of 4th instar larvae using the CTAB method (Chen et al., 2010). Promoters ranging from 0.5 to 1.1 kb fragments of selected genes were PCR amplified using the genomic DNA as the template and primers with restriction sites designed at the ends (underlined) (Table S3). Restricted PCR products were cloned into pGL3-Basic, a vector harboring the firefly luciferase (*LUC*) reporter gene (Promega, Madison, WI). Resulting constructs were sequenced for confirmation.

cis-Element deletions were accomplished by PCR with primers lacking the selected *cis*-element but containing its flanking regions. Two separate primary PCR products covered the promoter with an overlap region. Equal amounts (approximately 10 ng each) of purified PCR products via QIAquick gel extraction kit (Qiagen) were mixed and subjected to a secondary PCR to obtain the promoter without the *cis*-element. The secondary PCR products were subcloned into pGL3-Basic vector and sequences were confirmed as above.

2.8. Cloning of a putative transcription factor

The coding region of the putative cowpea bruchid zinc-finger homeodomain (*CmZFH*) was identified from our transcriptomic database. Due to its low copy number, the template cDNA was synthesized with a gene-specific primer, i.e. 2 μM *CmZFH*-R (Table S4), followed by amplification of the full coding region of *CmZFH* with primers *CmZFH*-F and *CmZFH*-R. KpnI and EcoRI, or EcoRI and HindIII restriction sites were introduced into the primers for subsequent directional cloning into

pAc5.1/V5-HisA (ThermoFisher Scientific, Waltham, MA) or pET28a vectors (Novagen, Madison, WI), respectively. The resulting constructs were sequence confirmed and putative structural domains were identified by SMART domain analysis (<http://smart.embl-heidelberg.de/>). Deletion constructs without the homeodomain or either of the zinc-finger clusters, i.e. *CmZFH* Δ HD, *CmZFH* Δ N-ZF and *CmZFH* Δ C-ZF were built as described previously and confirmed by DNA sequencing. Primers used were shown in Table S4.

2.9. Transient transfection and LUC assays

Drosophila Schneider 2 (S2) cells were maintained at 27°C in Shields and Sang M3 insect medium (Sigma) supplemented with 0.1% (w/v) yeast extract, 0.25% (w/v) bactopectone, 12.5% heat-inactivated fetal bovine serum, penicillin (50 U/mL), streptomycin (50 $\mu\text{g}/\text{mL}$) and fungizone (0.25 $\mu\text{g}/\text{mL}$). Cells were seeded in a 6-well plate (1×10^6 cells per well) and allowed to attach for 1 h. One μg of reporter plasmid and 0.2 μg of internal control plasmid pRL-SV40 (Promega) were introduced into the S2 cells with the calcium phosphate DNA precipitation method, and *LUC* assays were performed using the Dual-Luciferase Reporter 1000 Assay System (Promega) as previously described (Ahn et al., 2007, 2013). The transfection and *LUC* assays were performed at least 3 times.

To perform co-transfection, 0.2 μg of pAc5.1-*CmZFH* or its deletion mutants pAc5.1-*CmZFH* Δ N-ZF, pAc5.1-*CmZFH* Δ HD or pAc5.1-*CmZFH* Δ C-ZF was transfected into S2 cells together with the reporter plasmid, respectively. As the negative control, 0.2 μg of pAc5.1/V5-HisA vector was co-transfected with the reporter plasmid to ensure comparable total exogenous DNA in all co-transfection experiments.

2.10. Expressing functional recombinant *CmZFH* in bacteria

Sequence-confirmed constructs including pET28a-*CmZFH*, pET28a-*CmZFH* Δ N-ZF, pET28a-*CmZFH* Δ HD, pET28a-*CmZFH* Δ C-ZF and the empty vector pET28a were transformed into *E. coli* strain BL21/DE3, respectively. Induction and expression of recombinant proteins were accomplished as described previously (Cheng et al., 2020). Cells resuspended in 20 mL of 20 mM Tris-HCl (pH 7.5) were disrupted at 15,000 psi in a high-pressure homogenizer (EmulsiFlex-C3, Avestin, Canada). After a centrifugation at 15,000 rpm, 4°C for 25 min, the supernatant was discarded. The pellet (where the recombinant protein was located) was resuspended, spun down by a centrifugation as above, and redissolved in 1 mL of 6 M urea and incubated at 4°C for 3 h on an end-over-end rotator (~ 15 rpm), followed by centrifugation twice at 15,000 rpm, 4°C for 15 min to remove the insoluble substance. The supernatant was then filtered through a 4.5 μm filter before being transferred to the dialysis tubing with a MW cutoff of 12–14 kDa (Fisher scientific, Waltham, MA). Dialysis with stirring started in 3 M urea for 3 h, continued in urea solution with gradually decreased concentrations, followed by an overnight dialysis in 0.5 M urea. The tubing was then transferred to a 4 L dialysis buffer containing 2 mM MgCl_2 , 1 mM EDTA, 1 mM DTT and 20 mM Tris-HCl (pH 7.5) for 3 h and the dialysis buffer was changed twice. All dialyzing steps were performed at 4°C .

After dialysis, the soluble proteins were collected by a centrifugation at 15,000 rpm, 4°C for 15 min, and its concentration was determined by the Bradford assay. The presence of the recombinant protein was confirmed by western blotting using monoclonal mouse anti-His (1:1000 dilution, Qiagen) and horseradish peroxidase-conjugated goat anti-mouse IgG (1:5000 dilution, Sigma-Aldrich) as primary and secondary antibodies respectively.

Due to low expression levels of recombinant *CmZFH* and its variants, their *cis*-element binding activities were evaluated using resolubilized proteins with proper controls. Specifically, 5 μg of proteins were incubated with the radiolabeled probe *AREB6* in EMSA. For the supershift assays, 1 μL of the mouse anti-His monoclonal antibody was incubated with proteins for 20 min at room temperature prior to the addition of

probe.

2.11. Statistical analysis

All statistical analyses were performed with software SPSS 20.0 (IBM Corporation, Somers, NY). The Pearson correlation analysis was performed to compare fold changes in RNA-seq and RT-qPCR. Analysis of variance (ANOVA) followed by Tukey's test was used to evaluate the statistical significance in LUC activities in reporter constructs driven by various deletion promoters. Student's t-test was applied for comparison of LUC activities in the presence and absence of CmZFH, for analysis of relative gene expression under normoxia versus hypoxia. When comparing LUC activities between cells (expressing LUC reporter construct) co-transfected with intact CmZFH and with its various deletion forms as well as with empty expression plasmid, one-way ANOVA followed by Dunnett's post-hoc test was used to analyze statistical significance.

3. Results

3.1. Transcriptome assembly and hypoxia-responsive genes analysis

To investigate transcriptional response of cowpea bruchids to hypoxia, we performed RNA-seq using midguts of hypoxia-treated and control 4th instar larvae, respectively. After quality trimming, approximately 277 million reads generated by Illumina sequencing were assembled into 120,155 unigenes covering a total length of 111,969,312 bp. Unigenes, ranging from 224 to 32,100 bp, have an average length of 930 bp and an N50 of 1611 bp (Table S5, Fig. S1A). All unigenes were annotated against the NCBI non-redundant protein (Nr) database and 43,135 (35.6%) unigenes showed homology to the sequences in the Nr database.

Low O₂ stress caused significant expression changes of 602 genes, including 408 up- and 194 down-regulated genes, with a cutoff of $|\log_2(\text{fold change})| \geq 1$ and Q (the adjusted P -value) ≤ 0.05 (Table S6). To understand the function of these genes, we mapped them to the Gene Ontology (GO) and KEGG database. Overall, 259 hypoxia-responsive genes were functionally categorized into 53 GO terms (Fig. S1B) and 56 were functionally classified into 5 KEGG categories (Fig. S1C).

3.2. Identification of potential common hypoxia-responsive cis-elements

To begin to understand transcriptional co-regulation in response to hypoxia, we attempted to obtain promoter cis-regulatory elements common to up- or down-regulated genes. Among those that possessed GO terms or involved in KEGG pathways, 37 had the translation start codon and matched perfectly with genome DNA sequences. Of which, 20 were up-regulated and 17 were down-regulated. When validated by RT-qPCR, expression of these genes was highly consistent with results from transcriptome analysis ($R^2 = 0.8537$, $P < 0.0001$, Fig. 2). Also, we successfully obtained the 1 kb regions immediately upstream of the transcription start sites as putative promoters for these genes (Document S1).

Common TFs predicted 19 common cis-elements shared by induced genes and 18 common cis-elements shared by the repressed group from promoters of these hypoxia-responsive genes respectively, as well as their cognate putative binding proteins (Tables S7 and S8). It should be noted that each so-called putative common cis-element indeed contained multiple specific cis-elements from promoters of responsive genes. Common to these specific cis-elements was the conserved core sequence, but sequences adjacent to the core varied substantially although the requirement for the matrix similarity was met. When individually analyzing every cis-element sequence with MatInspector, we increased the cutoff stringency to narrow down associated cis-elements to a manageable number for EMSA tests (Fig. 1). As a result, AREB6, CHR, CDX2, CEBP, ABDB and SMARCA3 were selected as putative cis-

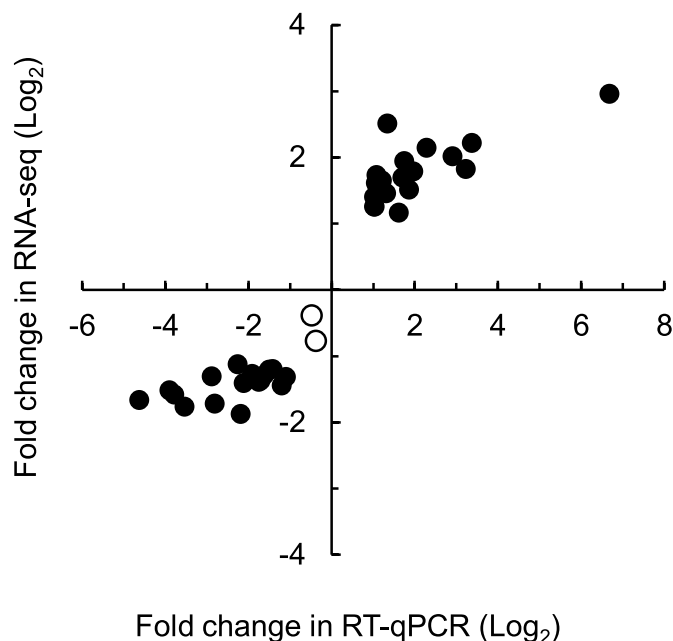


Fig. 2. RT-qPCR validation of selected hypoxia-responsive genes. Thirty-seven hypoxia-responsive genes (black dots) whose promoter sequences had been successfully identified in the genome database were subjected to RT-qPCR as described in Materials and Methods. Fold changes in RNA-seq and RT-qPCR were analyzed with the Pearson correlation analysis. The correlation coefficient (R^2) is 0.8537 ($P < 0.0001$). Two white dots represent negative control genes, i. e. unresponsive to hypoxia selected from RNA-seq.

elements potentially involved in co-regulation of hypoxia-responsive genes. While AREB6, CHR and CDX2 were present in promoters of up-regulated genes (Table S7), CEBP and ABDB existed in promoters of down-regulated genes (Table S8). Interestingly, SMARCA3 was found in promoters of both up- and down-regulated genes (Tables S7 and S8).

3.3. Differential binding of cis-elements by nuclear proteins of hypoxic insects

To determine whether these cis-elements were involved in insect response to hypoxia, we performed EMSAs using equal amount of nuclear extracts from midgut of normoxic and hypoxic larvae, judged by the Bradford protein assay and western blotting analysis (Data not shown). Stronger binding by hypoxic extract than normoxic extract to cis-elements AREB6, CDX2 and CEBP was observed in many promoters (Figs. S2A–C marked with *). The reverse was true for two ABDB-containing promoters (Fig. S2D). Such patterns suggested that AREB6 and CDX2 elements may interact with positive regulatory proteins and induce gene expression in response to hypoxia, whereas CEBP could interact with a repressor(s) leading to down-regulation of the target genes. ABDB may interact with an inducer(s) which expressed more highly in normoxic insects. Interestingly, opposite binding patterns were seen in CHR (Fig. S2E) as well as in SMARCA3 (Fig. S2F, marked with *), suggesting diverse interactions with nuclear binding proteins even though the same core sequence was shared. Elements showing no-binding or non-differential binding (without being labeled with * in Fig. S2) were not further pursued.

Competition assays, i. e. applying excess of unlabeled specific probes to interrupt interactions between P-32 labeled 'hot' probes and their corresponding binding proteins, confirmed specific binding of the following cis-elements (Fig. 3, marked with *): AREB6 from *CmScylla*, *CmLPCAT* and *CmDYRK2* (Fig. 3A), CDX2 from *CmL-GalDH* (Fig. 3B), CEBP from *CmGPCPD1* (Fig. 3C), ABDB from *CmHSP60* (Fig. 3D), CHR from *CmE63-1*, *CmPKA* and *CmCatB* (Fig. 3E), and SMARCA3 from

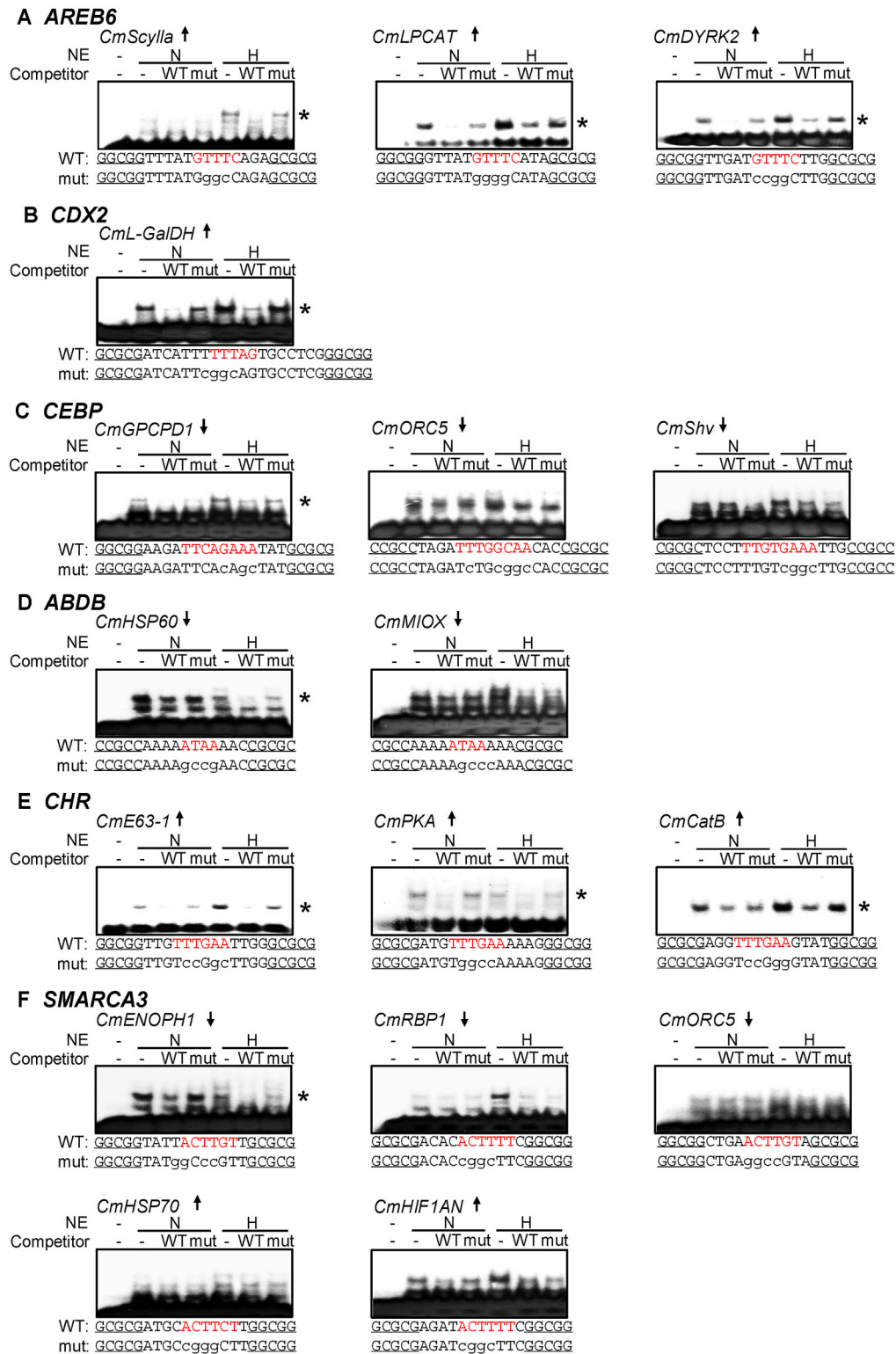


Fig. 3. Differential interaction of midgut nuclear extracts of normoxic and hypoxic larvae with selected cis-elements. Nuclear extract was incubated with each of the γ -³²p labeled cis-element probes: (A) AREB6, (B) CDX2, (C) CEBP, (D) ABDB, (E) CHR and (F) SMARCA3. DNA binding specificity was tested by adding excess of the unlabeled wild-type probe (WT) or unlabeled mutated probe (mut). NE: midgut nuclear extract from normoxic 4th instar larvae (N) or 24 h hypoxia-treated 4th instar larvae (H). *CmLPCAT*: lysophosphatidylcholine acyltransferase; *CmDYRK2*: dual-specificity tyrosine phosphorylation-regulated kinase 2; *CmL-GalDH*: L-galactose dehydrogenase; *CmGPCPD1*: glycerophosphocholine phosphodiesterase 1; *CmORC5*: origin recognition complex subunit 5; *CmShv*: shriveled; *CmHSP60*: heat shock protein 60; *CmMIOX*: myo-inositol oxygenase; *CmE63-1*: calcium-binding protein E63-1; *CmPKA*: cAMP-dependent protein kinase; *CmCatB*: cathepsin-B like proteases; *CmENOPH1*: enolase-phosphatase E1; *CmRBP1*: RNA-binding protein 1; *CmHSP70*: heat shock protein 70; *CmHIF1AN*: hypoxia-inducible factor 1 α -subunit inhibitor. Hypoxia-induced and -repressed genes are marked as \uparrow and \downarrow , respectively next to the gene names. GC-rich sequences (underlined) were added to both ends of every probe to ensure double helix formation after annealing. Specific DNA-protein complexes are indicated by asterisks (*). Core binding sequences are marked red, and altered nucleotides are expressed as lowercase letters. (For interpretation of the references to color in this figure legend, the reader is referred to the Web version of this article.)

CmENOPH1 (Fig. 3F). Binding to *CEBP* from *CmORC5* and *CmShv* (Fig. 3C), *ABDB* from *CmMIOX* (Fig. 3D), and *SMARCA3* from *CmRBP1*, *CmORC5*, *CmHSP70* and *CmHIF1AN* (Fig. 3F) turned out to be non-specific.

3.4. Regulatory activities of cis-elements in corresponding promoters

To illustrate the significance of these cis-elements in hypoxia-responsive gene regulation, we first cloned individual putative

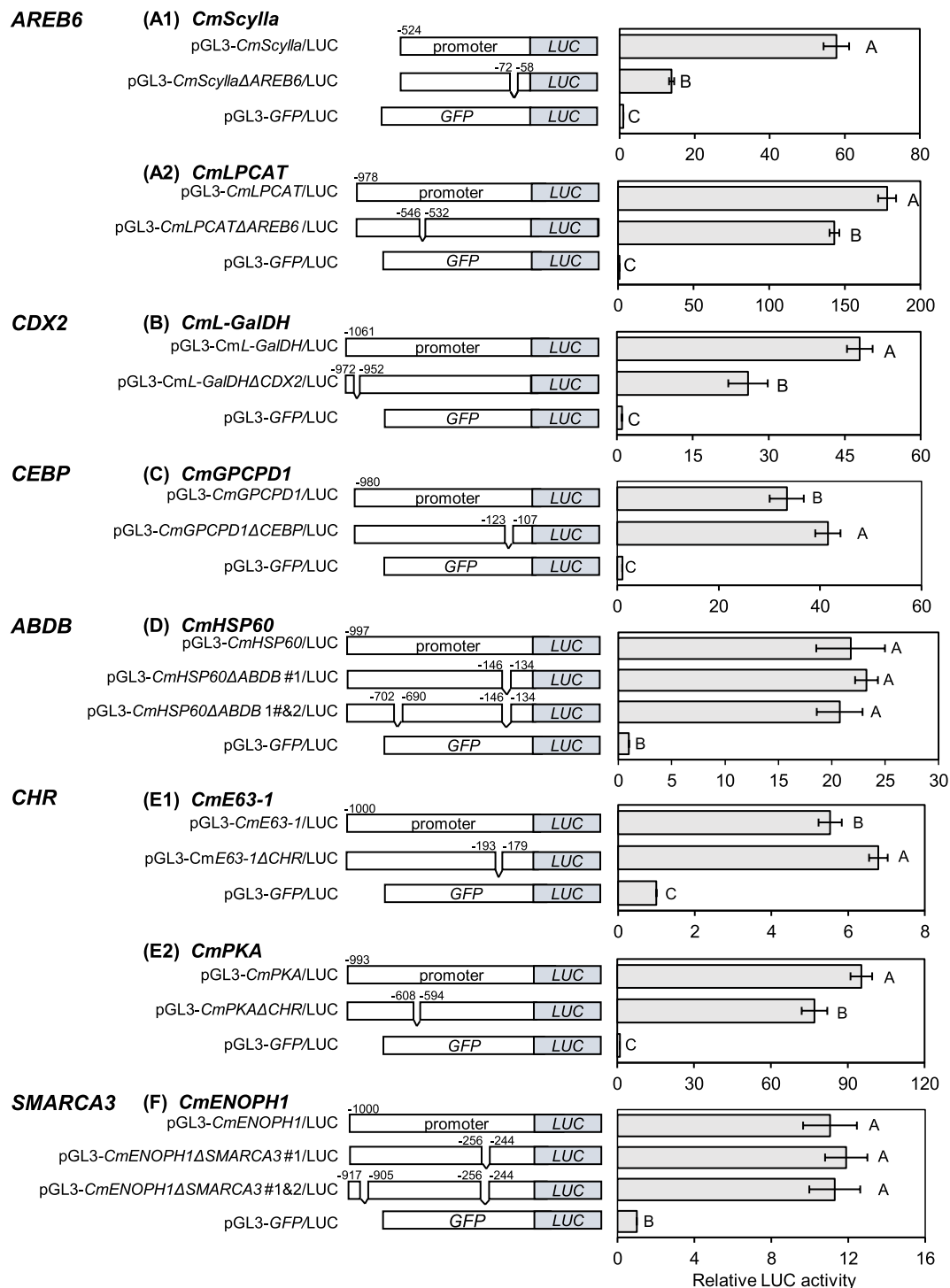


Fig. 4. Promoter deletion analysis. Left panel: schematic diagrams of promoters with or without cis-element(s) that displayed differential binding in EMSAs (Fig. 3, marked with *). Negative numbers are relative to the putative transcription initiation site (+1). Right panel: relative reporter LUC activities driven by corresponding promoter variants. Promoter and GFP fragments were ligated into pGL3-Basic vector that harbored LUC reporter gene, and transfected to S2 cells, respectively. *Renilla* luciferase plasmid pRL-SV40 served as an internal control. Relative LUC activity (mean \pm S.E.) was expressed as fold induction relative to that of the GFP control. Different letters indicate significant difference among different reporter constructs (one-way ANOVA followed by Tukey's test, $n = 3$, $P < 0.05$). *CmScylla* (A1); *CmLPCAT*: lysophosphatidylcholine acyltransferase (A2); *CmL-GalDH*: L-galactose dehydrogenase (B); *CmGPCPD1*: glycerophosphocholine phosphodiesterase 1 (C); *CmHSP60*: heat shock protein 60 (D); *CmE63-1*: calcium-binding protein E63-1 (E1); *CmPKA*: cAMP-dependent protein kinase (E2); *CmENOPH1*: enolase-phosphatase E1 (F).

promoter regions into the pGL3-Basic luciferase (LUC) reporter vector. Upon transient transfection into *Drosophila* S2 cells, cells with pGL3-promoter/LUC constructs emitted significantly higher luminescence than the non-promoter control pGL3-GFP/LUC ($P < 0.05$, Fig. 4), illustrating their promoter function. Removal of *AREB6* or *CDX2* elements from the corresponding promoters, however, caused drastic reduction of the LUC activity ($P < 0.05$, Fig. 4A1-2, 4B), suggesting that they were essential components for gene activation, consistent with results from EMSAs (Fig. 3). Conversely, deletion of *CEBP* from the *CmGPCPD1* promoter resulted in increased LUC activity ($P < 0.05$, Fig. 4C), indicating its interaction with a repressor. Interestingly, removing *CHR* from different promoters resulted in either increased (*CmE63-1*) or decreased (*CmPKA*) LUC activity ($P < 0.05$, Fig. 4E1-2), consistent with the binding patterns shown in EMSAs. Most likely, the *CHR*-element could recruit diverse factors to either repress or activate gene expression. No change however, was observed when we deleted all possible *ABDB* and *SMARCA3* elements from the promoter sequences of *CmHSP60* and *CmENOPH1*, respectively (Fig. 4D and 4F), suggesting the existence of other *cis*-regulatory elements.

3.5. *CmZFH* transcription factor interacted with *AREB6*-element to activate *CmScylla* and *CmLPCAT* expression

The aforementioned results suggested that *AREB6* may coordinately induce expression of hypoxia-responsive genes, *CmScylla* and *CmLPCAT*. The MatInspector software predicted a zinc-finger homeodomain (ZFH) transcription factor as the putative *AREB6*-binding protein (Table S7). ZFH from *Drosophila* (DmZFH-1) is involved in the development of the embryonic central nervous system, embryonic mesoderm and adult musculature (Lai et al., 1991), as well as in regulation of immune response (Myllymaki and Ramet, 2013). The human homolog ZEB1 controls epithelial-mesenchymal cell type transition, an essential process throughout embryonic morphogenesis (Hutchins and Bronner, 2021). In addition, it acts as an important molecule to regulate DNA damage and cancer cell differentiation (Drapela et al., 2020). Members in the ZFH family contain zinc-finger clusters in both N- and C-terminal

regions and a homeodomain in between (Li et al., 2021). All zinc-fingers share the consensus sequence of (F/Y)XCX₂₋₄CX₃(F/Y)X₅LX₂HX₃₋₅H (Laity et al., 2000), whereas all homeodomains contain a helix-turn-helix structure with the conserved residues (R/G)X₆QX₃(L/V)X₃(F/Y)X₁₉(L/N)X₄(V/I)X₂WFXNXRX(R/K)X(R,K) (Scott et al., 1989).

To determine the molecular property and function of the *AREB6*-binding protein in cowpea bruchids, we searched the transcriptome and cloned the bruchid ZFH (*CmZFH*). It encoded a protein of 961 amino acid residues with nine zinc-finger and one homeodomain motifs (Fig. S3A). Sequence alignment showed rather high sequence similarity in these conserved domain regions with homologs from other species (Fig. S3B).

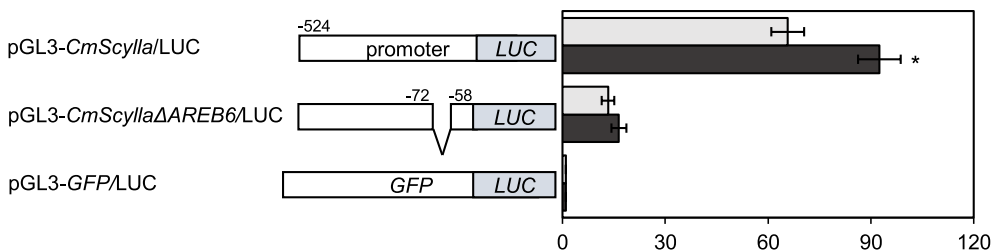
To determine whether *CmZFH* could bind to the *AREB6* element and co-regulate hypoxia-responsive genes, we co-transfected S2 cells with the expression construct pAc5.1-*CmZFH* and the reporter plasmid harboring *CmScylla* or *CmLPCAT* promoter, i.e. pGL3-*CmScylla*/LUC or pGL3-*CmLPCAT*/LUC. Apparently, *CmZFH* effectively activated *CmScylla* and *CmLPCAT* expression, but this induction was abolished if the *cis*-element *AREB6* was deleted from their promoters ($P < 0.05$, Fig. 5). In the case of *CmLPCAT* promoter, it seems multiple *AREB6* elements contributed to its full induction, with the #2 *AREB6* (-545 to -533 bp, the same as shown in Fig. 4A2) being the major *cis*-regulator. Overall, *CmZFH* could exert its transcriptional activator function to co-regulate the expression of *CmScylla* and *CmLPCAT* through its interaction with the common promoter element *AREB6*.

We performed RT-qPCR to examine the transcript abundance of *CmZFH* and its two target genes *CmScylla* and *CmLPCAT* after 4, 8 and 24 h hypoxia treatment, respectively. *CmZFH* was significantly induced at the 4 and 8 h time points but induction faded by 24 h. Induction of *CmScylla* was only seen at 24 h whereas *CmLPCAT* was significantly induced at all time points ($P < 0.05$, Fig. 6).

3.6. *CmZFH* transcription factor bound to *cis*-element *AREB6* via the N-terminal zinc-finger cluster

The DNA-binding property via the zinc-finger clusters and/or the homeodomain has been demonstrated in many ZFH family members

CmScylla



CmLPCAT

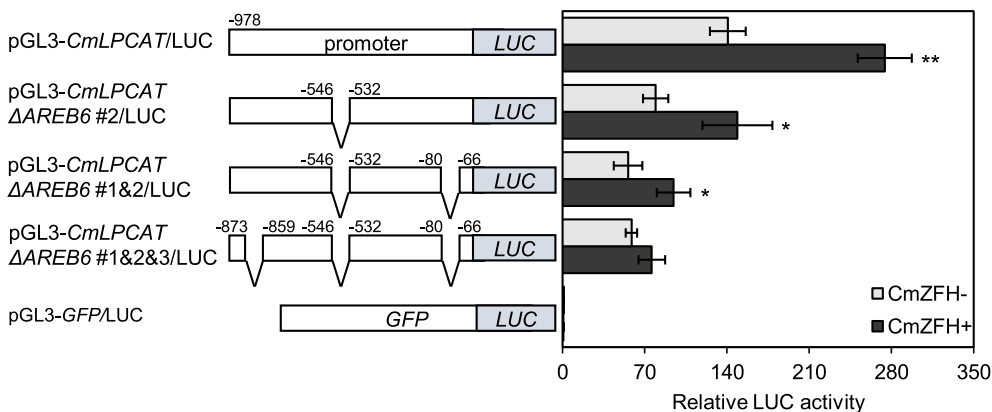


Fig. 5. *CmZFH* activated transcription of *CmScylla* and *CmLPCAT* through interaction with *AREB6* in their promoters. S2 cells were co-transfected with a reporter plasmid (LUC driven by one of the promoter variants shown) and *CmZFH*-expressing pAc5.1-*CmZFH* (black bars) or *CmZFH*-null empty vector control (grey bars). *Renilla* luciferase plasmid pRL-SV40 served as the internal control. Relative LUC activity (mean ± S.E.) was expressed as fold induction relative to that of the GFP control without *CmZFH*. Asterisks indicate significant difference in relative LUC activity in the presence versus absence of *CmZFH* (t-test, $n = 3$, *: $P < 0.05$, **: $P < 0.01$). *CmLPCAT*: lysophosphatidylcholine acyltransferase.

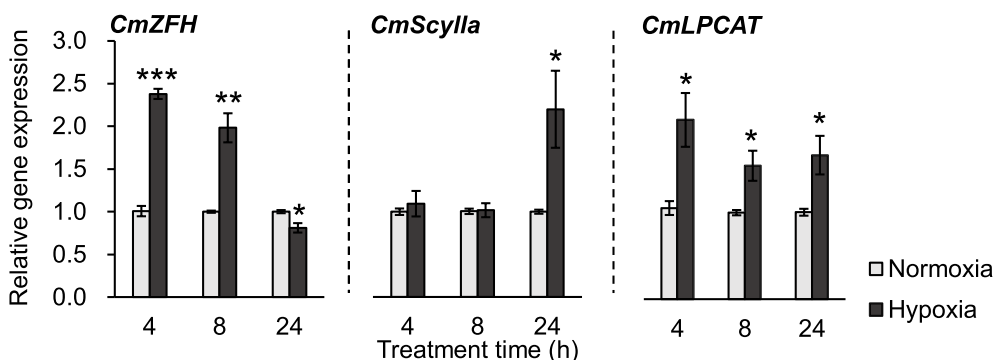


Fig. 6. Hypoxia induced expression of CmZFH and its targets CmScylla and CmLPCAT. The 4th instar larvae were subjected to hypoxia treatment for 4, 8 and 24 h, respectively. Gene expression levels determined by RT-qPCR were relative to those of the normoxic counterparts. *18S rRNA* was used as the internal control. Significant difference in relative gene expression at each time point was determined by the student's t-test. n = 3, *: $P < 0.05$, **: $P < 0.01$, ***: $P < 0.001$.

(Ikeda and Kawakami, 1995; Postigo and Dean, 1999; Sekido et al., 1997). To locate the interacting domain(s) in CmZFH, we bacterially expressed the CmZFH protein and its variants with putative DNA-binding domains individually deleted (Fig. 7A). Since zinc-fingers 1 and 6 were not conserved in all homologs (Fig. S3), they remained intact in zinc-finger cluster deletion experiments. Because the recombinant proteins were found in inclusion bodies, we performed urea-denaturation and gradual renaturation and successfully gained their solubility.

We chose the *CmScylla* promoter element to study molecular interaction between CmZFH and the *AREB6*-element. EMSAs demonstrated the DNA-binding activity of the intact protein, an activity that was absent in the negative controls, i.e. the empty vector and the uninduced construct (Fig. 7B). Anti-His antibody disrupted the CmZFH-*AREB6* complex, which was yet another evidence confirming their specific interaction. Binding to *AREB6* was abolished when the zinc-finger cluster at the N-terminus was deleted (Δ N-ZF), but unaffected when the homeodomain (Δ Hd) or the zinc-finger cluster at the C-terminus (Δ C-ZF) was removed (Figs. 7B and S4).

In co-transfection assays, only CmZFH that lacked N-ZF failed to

further enhance the basal promoter activity ($P < 0.05$, Fig. 8), consistent with binding results obtained from the recombinant proteins. Therefore, the N-terminal zinc-finger cluster most likely was responsible for *AREB6*-binding, through which CmZFH interacted with *CmScylla* promoter.

4. Discussion

The importance of transcriptional abundance in shaping insect adaptive response to hypoxia has been well known, but the regulatory mechanisms, particularly in underrepresented non-model storage pests, remain to be investigated. Inspired by the discovery that a single transcription factor (i.e. hairy) in hypoxic *Drosophila* is able to coordinate the expression of a group of metabolic genes in the TCA cycle (Zhou et al., 2008), we attempted to gain more insight into the regulatory network underlying hypoxia tolerance through the current research. Ultimately, these upstream regulators could become the targets in our effort of optimizing the strategy to control storage pests.

Exposure of cowpea bruchids to low O_2 led to coordinated regulation of diverse gene sets. We retrieved promoter sequences of 37 hypoxia-

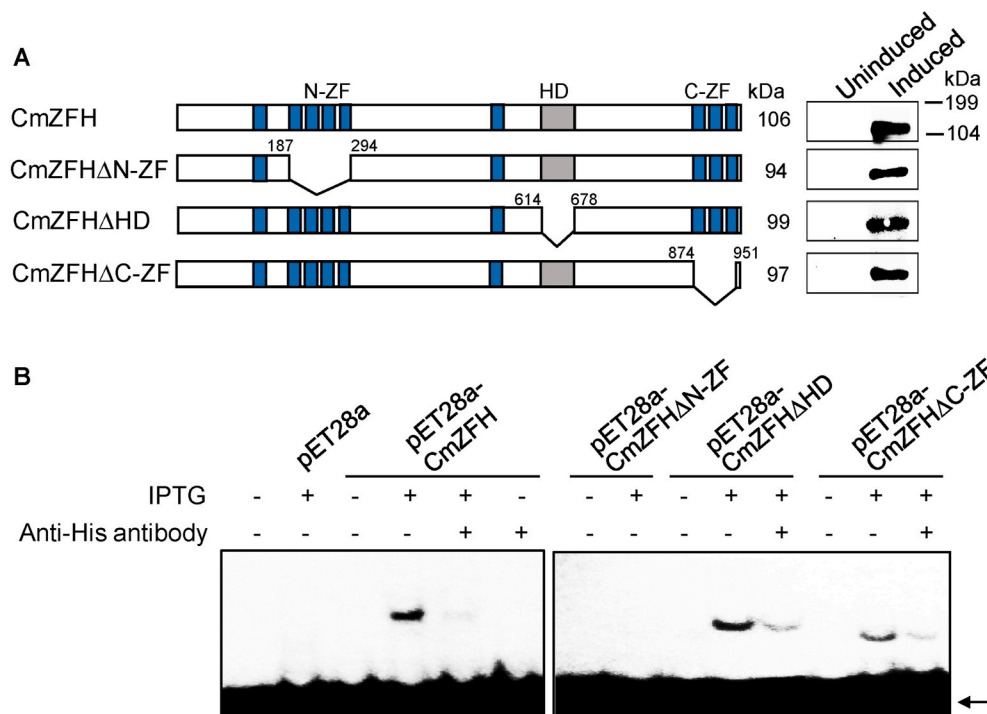


Fig. 7. CmZFH specifically interacted with cis-element AREB6 via the N-terminal zinc-finger cluster (N-ZF). (A, left panel) Diagrams of CmZFH and its deletion variants. Numbers above diagrams indicate the amino acid positions at deletion sites. The insoluble bacterially expressed recombinant proteins after IPTG induction were denatured in urea and gradually renatured by dialysis. Soluble proteins were used for western blotting (A, right panel) with anti-His antibody. (B) Recombinant CmZFH lacking the N-terminal zinc-finger cluster (CmZFH Δ N-ZF) failed to bind *AREB6* from the promoter of *CmScylla*. Arrows mark the γ - ^{32}P labeled free *AREB6* probe. Both IPTG-induced empty vector and uninduced expression constructs (pET28a-CmZFH, pET28a-CmZFH Δ N-ZF, pET28a-CmZFH Δ Hd, pET28a-CmZFH Δ C-ZF) served as negative controls to exclude the possibility of interaction being non-specific. N-ZF: N-terminal zinc-finger cluster, i.e. the conserved #2–5 zinc fingers; HD: homeodomain; C-ZF: C-terminal zinc-finger cluster, i.e. the conserved #7–9 zinc fingers.

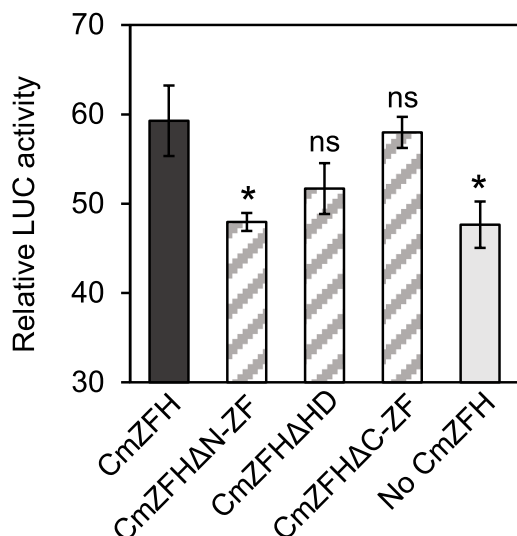


Fig. 8. Deletion of the N-terminal zinc-finger cluster abolished transcriptional activation activity of CmZFH. S2 cells were co-transfected with LUC reporter plasmid (pGL3-*CmScylla*) and expression plasmid (CmZFH or its deletion variants CmZFHΔN-ZF, CmZFHΔHD, CmZFHΔC-ZF) or equivalent empty expression vector. *Renilla* luciferase plasmid pRL-SV40 served as an internal control. Relative LUC activity (mean ± S.E.) was expressed as fold induction relative to that of the *GFP* control without CmZFH. Asterisks indicate significant difference compared to the intact CmZFH control (one-way ANOVA with Dunnett's post-hoc test, $n = 4$, *: $P < 0.05$, ns: no significance).

responsive genes and identified putative common *cis*-elements for induced and repressed groups respectively, according to the scoring algorithm defined in Fig. 1. In the follow-up confirmation experiments, our hypothesis was that genes co-regulated under certain biological context, i.e. endurance of low O₂ availability, share common promoter elements and transcriptional regulators. We discovered a novel transcription factor co-regulating at least two hypoxia-induced genes based on the conservation of the cognate *cis*-element, and experimentally verified its transcriptional activation activity. Therefore, common *cis*-element analysis can lead to better understanding of the orchestration of gene networks.

Despite the success, many factors may contribute to the low prediction rate of 'true' *cis*-elements. Simply possessing a *cis*-element-like sequence apparently could not warrant its regulatory function. Many promoter elements initially identified were gradually excluded from further investigation during experimental confirmation steps. For example, some were unable to demonstrate differential or specific binding in EMSA, and others failed to illustrate *cis*-regulatory activity in promoter analysis. Furthermore, it is commonly known that an individual element often contains overlapping binding specificities for different classes of transcription factors. To minimize confusion, we only focused on those elements that had single hits, which likely eliminated many possible candidates. To address transcriptional co-regulation, we did not pursue those *cis*-elements whose regulatory functions had been confirmed in only one gene (e.g. *CEBP*). We also did not pursue the *CHR* element: when deleted from promoters of *CmE63-1* and *CmPKA* (both hypoxia-induced), opposite binding patterns in EMSA and LUC activities (Figs. 3E and 4E) reflected a complicated regulation. It is possible that its putative binding protein LIN54, a component of the MuvB complex (Marceau et al., 2016), recruited different co-factors to manipulate gene expression as previously described (Engeland, 2018; Sadasivam et al., 2012). Additionally, diverse DNA sequences beyond the highly conserved *cis*-element core forced us to individually confirm each promoter *cis*-element for differential nuclear protein binding. This inevitably posed a limit to the number of potentially co-regulated genes that could be practically tested. Perhaps focusing on genes in a single

metabolic pathway or related functional complexes as Zhou et al. (2008) would decrease false positive *cis*-element predictions. Increasing the selection stringency for genes sharing similar spatial and/or temporal expression patterns across the experimental condition as in studies by (Yu et al., 2015) should also improve the efficiency of collecting truly co-regulated target genes.

Not all co-expressed genes are necessarily co-regulated. Growing evidence suggests that the influence of a promoter *cis*-regulatory element on gene expression is controlled by combinatorial factors: For a given *cis*-element, its orientation and its distance to the translation start site ATG, as well as the order and spacing relative to other elements all play key roles in transcriptional regulation of target genes (Beer and Tavazoie, 2004; Cohen et al., 2006; Fessele et al., 2002). Presumably, analysis of the relative organization of some elements within a promoter, rather than mere detection of the presence of a common element alone, is more efficient and reliable bioinformatics-based approach for studying co-regulation of hypoxia-responsive genes. Knowledge about the promoter framework should help reduce effort on non-functional *cis*-elements.

Nevertheless, our approach did successfully recognize the transcriptional activation activity of CmZFH and established its novel co-regulator function in response to low O₂. This transcription factor is featured by two zinc-finger clusters separated by a homeodomain (Fig. S3). These domains have been shown previously to possess DNA-binding activity. Gel-shift and transient transfection assays suggested that CmZFH regulated transcriptional expression through interacting with *AREB6* via its N-terminal zinc-finger cluster (Figs. 7 and 8). This is intriguing because homologs of CmZFH are reported to bind to *cis*-elements with a CACCT core, known as the *E*-box, via both zinc-finger clusters (Ikeda and Kawakami, 1995; Postigo et al., 1999; Sekido et al., 1997). Interestingly, Ikeda and Kawakami (1995) discovered that probes containing an *E*-box in conjunction with the consensus sequence GTTTC/G, i.e. the so called the *AREB6* element, strengthen binding to the *E*-box by the N-terminal zinc-finger cluster. Here, using genomics, bioinformatics and molecular tools, we demonstrated that the N-terminal zinc-finger cluster of CmZFH indeed directly bound to *AREB6*, and such interaction enhanced expression of hypoxia-responsive genes. For the first time, our finding renders *AREB6* the binding site of CmZFH, beyond its reported role as an interacting facilitator. Notably, an *E*-box was present 53 bp downstream the *AREB6* site in the *CmScylla* promoter, but absent in the *CmLPCAT* promoter region. Further experiments are needed to determine if *AREB6* is a common target for the ZFH family. Conversely, information on whether CmZFH could bind to the *E*-box, and the potential mutual influence between the two *cis*-elements should also be obtained. Moreover, it would be interesting to know domain interactions within CmZFH and whether CmZFH can recruit different co-factors through different regions to activate or repress downstream gene expression as its vertebrate homologs (Bruneel et al., 2020; Fukagawa et al., 2015; Furusawa et al., 1999; Lehmann et al., 2016; Nishimura et al., 2006; Postigo and Dean, 1999; Postigo et al., 2003).

CmZFH activated the expression of *CmLPCAT* and *CmScylla* under hypoxia (Fig. 5). *Scylla*, existing throughout the animal kingdom, is an important protein under hypoxic conditions (Brugarolas et al., 2004; Reiling and Hafen, 2004; Shoshani et al., 2002). In human, mouse and *Drosophila*, *Scylla* and homologs/paralogs are induced by various cellular stresses including DNA damage and hypoxia. *Scylla*-over-expressing *Drosophila* display growth inhibition, whereas loss of *Scylla* function causes overgrowth in flies under normoxia but renders them more susceptible to low O₂ (Reiling and Hafen, 2004). The up-regulation of *CmScylla* upon hypoxia treatment (Fig. 6) suggest a similar growth repressor role played by the homologous protein in cowpea bruchid, which may account partly for the retarded development of hypoxic bruchid larvae. Yet, such a growth inhibitory function presumably is crucial for their endurance of prolonged hypoxia. Interestingly, *CmScylla* in mammals and *Drosophila* is directly targeted by HIF1, a well-known heterodimeric transcription factor (Brugarolas et al., 2004; Reiling and

Hafen, 2004; Shoshani et al., 2002). Although we also demonstrated previously that CmHIF1 regulated expression of the hypoxia-induced genes *CmHSP21* and *CmHSP27* (Ahn et al., 2013), HIF1-binding site was not found in the 2 kb region upstream of the transcription initiation site of *CmScylla*. Therefore, this gene in cowpea bruchids most likely was not regulated by CmHIF1, but by CmZFH. Actually, it is not uncommon that a given gene in different species is controlled by different transcription factors. For instance, the hypoxia-induced gene phosphofructokinase (*PFK*) is regulated by HIF1 in the white shrimp *Litopenaeus vannamei* (Cota-Ruiz et al., 2016). However, it is regulated instead by an estrogen-related receptor (dERR) in *Drosophila* larvae (Li et al., 2013).

The lysophosphatidylcholine acyltransferase gene (*CmLPCAT*), also induced under hypoxia, possibly shares the same regulator as *CmScylla* (Fig. 6). It is shown in human colorectal cancer cells that production of lipid droplet is driven by LPCAT2. The LPCAT2-induced lipid droplet biogenesis promotes ER homeostasis and prevents cell death (Cotte et al., 2018). Interestingly, hypoxic *Drosophila* larvae increase their fat body lipid droplet production and this altered lipid metabolism is needed for hypoxia tolerance (Lee et al., 2019). Although *CmLPCAT* was cloned from the midgut tissue, it could contribute to organismal adaptation to hypoxia, leading to prolonged life span. Further experiments are necessary to determine the role of *CmLPCAT* in enhancing insect survival under hypoxia.

5. Conclusion

Revealing regulatory networks is key to understanding molecular mechanism of hypoxia tolerance in insect pests. Our research has demonstrated the feasibility of using common promoter *cis*-element analysis to identify novel insect transcription factors and shed more light into the co-regulation network associated with hypoxia. To our knowledge, this is the first time that CmZFH has been recognized for its role as one of the upstream regulators in insect adaptation to hypoxic environments. Information on molecular regulation of hypoxia-responsive genes will increase our understanding of how cowpea bruchids survive hypoxic stress and can potentially facilitate future storage pest control.

Author contributions

LH, CLL, KZS: designed the manuscript, LH, ZZ, WPZ, LW, JXL: transcriptome analysis; AS and GA: promoter identification; LH, IWC, WS, RJ: conducted the experiments; LH, KZS: wrote the manuscript.

Funding

This work was supported by the USDA-NIFA grant (2014-67013-21781) and China Scholarship Council.

Declaration of competing interest

The authors declare no competing interest.

Appendix A. Supplementary data

Supplementary data to this article can be found online at <https://doi.org/10.1016/j.ibmb.2021.103681>.

References

- Abdelrahman, H., Rinehart, J.P., Yocum, G.D., Greenlee, K.J., Helm, B.R., Kemp, W.P., Schulz, C.H., Bowsler, J.H., 2014. Extended hypoxia in the alfalfa leafcutting bee, *Megachile rotundata*, increases survival but causes sub-lethal effects. *J. Insect Physiol.* 64, 81–89. <https://doi.org/10.1016/j.jinsphys.2014.03.007>.
- Ahn, J.E., Guarino, L.A., Zhu-Salzman, K., 2007. Seven-up facilitates insect counter-defense by suppressing cathepsin B expression. *FEBS J.* 274, 2800–2814. <https://doi.org/10.1111/j.1472-4658.2007.05816.x>.
- Ahn, J.E., Guarino, L.A., Zhu-Salzman, K., 2010. Coordination of hepatocyte nuclear factor 4 and seven-up controls insect counter-defense cathepsin B expression. *J. Biol. Chem.* 285, 6573–6584. <https://doi.org/10.1074/jbc.M109.095596>.
- Ahn, J.E., Zhou, X., Dowd, S.E., Chapkin, R.S., Zhu-Salzman, K., 2013. Insight into hypoxia tolerance in cowpea bruchid: metabolic repression and heat shock protein regulation via hypoxia-inducible factor 1. *PLoS One* 8, e57267. <https://doi.org/10.1371/journal.pone.0057267>.
- Barretto, E.C., Polan, D.M., Beevor-Potts, A.N., Lee, B., Grewal, S.S., 2020. Toleranceto hypoxia is promoted by FOXO regulation of the innate immunity transcription factor NF- κ B/Relish in *Drosophila*. *Genetics* 215, 1013–1025. <https://doi.org/10.1534/genetics.120.303219>.
- Beer, M.A., Tavazoie, S., 2004. Predicting gene expression from sequence. *Cell* 117, 185–198. [https://doi.org/10.1016/s0092-8674\(04\)00304-6](https://doi.org/10.1016/s0092-8674(04)00304-6).
- Bradford, M.M., 1976. A rapid and sensitive method for the quantitation of microgram quantities of protein utilizing the principle of protein-dye binding. *Anal. Biochem.* 72, 248–254. <https://doi.org/10.1006/abio.1976.9999>.
- Brugarolas, J., Lei, K., Hurley, R.L., Manning, B.D., Reiling, J.H., Hafen, E., Witters, L.A., Ellisen, L.W., Kaelin Jr., W.G., 2004. Regulation of mTOR function in response to hypoxia by REDD1 and the TSC1/TSC2 tumor suppressor complex. *Genes Dev.* 18, 2893–2904. <https://doi.org/10.1101/gad.1256804>.
- Bruneel, K., Verstepp, J., Vandamme, N., Berx, G., 2020. Intrinsic balance between ZEB family members is important for melanocyte homeostasis and melanoma progression. *Cancers* 12. <https://doi.org/10.3390/cancers12082248>.
- Buttgereit, F., Brand, M.D., 1995. A hierarchy of ATP-consuming processes in mammalian cells. *Biochem. J.* 312 (Pt 1), 163–167. <https://doi.org/10.1042/bj3120163>.
- Cartharius, K., Frech, K., Grote, K., Klocke, B., Haltmeier, M., Klingenhoff, A., Frisch, M., Bayerlein, M., Werner, T., 2005. MatInspector and beyond: promoter analysis based on transcription factor binding sites. *Bioinformatics* 21, 2933–2942. <https://doi.org/10.1093/bioinformatics/bti473>.
- Centanin, L., Dekanty, A., Romero, N., Irisarri, M., Gorr, T.A., Wappner, P., 2008. Cell autonomy of HIF effects in *Drosophila*: tracheal cells sense hypoxia and induce terminal branch sprouting. *Dev. Cell* 14, 547–558. <https://doi.org/10.1016/j.devcel.2008.01.020>.
- Chen, H., Rangasamy, M., Tan, S.Y., Wang, H., Siegfried, B.D., 2010. Evaluation of five methods for total DNA extraction from western corn rootworm beetles. *PLoS One* 5, e11963. <https://doi.org/10.1371/journal.pone.0011963>.
- Cheng, W., Lei, J., Ahn, J.E., Liu, T.X., Zhu-Salzman, K., 2012. Effects of decreased O₂ and elevated CO₂ on survival, development, and gene expression in cowpea bruchids. *J. Insect Physiol.* 58, 792–800. <https://doi.org/10.1016/j.jinsphys.2012.02.005>.
- Cheng, W., Zhang, Y., Yu, J., Liu, W., Zhu-Salzman, K., 2020. Functional analysis of odorant-binding proteins 12 and 17 from wheat blossom midge sitodiplosis mosellana Gehin (Diptera: Cecidomyiidae). *Insects* 11. <https://doi.org/10.3390/insects11120891>.
- Cohen, C.D., Klingenhoff, A., Boucherot, A., Nitsche, A., Henger, A., Brunner, B., Schmid, H., Merkle, M., Saleem, M.A., Koller, K.P., Werner, T., Grone, H.J., Nelson, P.J., Kretzler, M., 2006. Comparative promoter analysis allows de novo identification of specialized cell junction-associated proteins. *Proc. Natl. Acad. Sci. U. S. A.* 103, 5682–5687. <https://doi.org/10.1073/pnas.0511257103>.
- Cota-Ruiz, K., Leyva-Carrillo, L., Peregrino-Urriarte, A.B., Valenzuela-Soto, E.M., Gollas-Galvan, T., Gomez-Jimenez, S., Hernandez, J., Yepiz-Plascencia, G., 2016. Role of HIF-1 on phosphofructokinase and fructose 1, 6-bisphosphatase expression during hypoxia in the white shrimp *Litopenaeus vannamei*. *Comp. Biochem. Physiol. Mol. Integr. Physiol.* 198, 1–7. <https://doi.org/10.1016/j.cbpa.2016.03.015>.
- Cotte, A.K., Aires, V., Fredon, M., Limagne, E., Derangere, V., Thibaudin, M., Humblin, E., Scagliarini, A., de Barros, J.P., Hillon, P., Ghiringhelli, F., Delmas, D., 2018. Lysophosphatidylcholine acyltransferase 2-mediated lipid droplet production supports colorectal cancer chemoresistance. *Nat. Commun.* 9, 322. <https://doi.org/10.1038/s41467-017-02732-5>.
- Crooks, G.E., Hon, G., Chandonia, J.M., Brenner, S.E., 2004. WebLogo: a sequence logo generator. *Genome Res.* 14, 1188–1190. <https://doi.org/10.1101/gr.849004>.
- Drapela, S., Bouchal, J., Jolly, M.K., Culig, Z., Soucek, K., 2020. ZEB1: a critical regulator of cell plasticity, DNA damage response, and therapy resistance. *Front. Mol. Biosci.* 7, 36. <https://doi.org/10.3389/fmolb.2020.00036>.
- Engeland, K., 2018. Cell cycle arrest through indirect transcriptional repression by p53: I have a DREAM. *Cell Death Differ.* 25, 114–132. <https://doi.org/10.1038/cdd.2017.172>.
- Farzin, M., Albert, T., Pierce, N., VandenBrooks, J.M., Dodge, T., Harrison, J.F., 2014. Acute and chronic effects of atmospheric oxygen on the feeding behavior of *Drosophila melanogaster* larvae. *J. Insect Physiol.* 68, 23–29. <https://doi.org/10.1016/j.jinsphys.2014.06.017>.
- Fessele, S., Maier, H., Zischek, C., Nelson, P.J., Werner, T., 2002. Regulatory context is a crucial part of gene function. *Trends Genet.* 18, 60–63. [https://doi.org/10.1016/s0168-9525\(02\)02591-x](https://doi.org/10.1016/s0168-9525(02)02591-x).
- Fukagawa, A., Ishii, H., Miyazawa, K., Saitoh, M., 2015. δ EF1 associates with DNMT1 and maintains DNA methylation of the E-cadherin promoter in breast cancer cells. *Canc. Med.* 4, 125–135. <https://doi.org/10.1002/cam4.347>.
- Furusawa, T., Moribe, H., Kondoh, H., Higashi, Y., 1999. Identification of CtBP1 and CtBP2 as corepressors of zinc finger-homeodomain factor δ EF1. *Mol. Cell Biol.* 19, 8581–8590. <https://doi.org/10.1128/mcb.19.12.8581>.
- Gorr, T.A., Gassmann, M., Wappner, P., 2006. Sensing and responding to hypoxia via HIF in model invertebrates. *J. Insect Physiol.* 52, 349–364. <https://doi.org/10.1016/j.jinsphys.2006.01.002>.
- Harrison, J.F., Greenlee, K.J., Verberk, W., 2018. Functional hypoxia in insects: definition, assessment, and consequences for physiology, ecology, and evolution.

- Annu. Rev. Entomol. 63, 303–325. <https://doi.org/10.1146/annurev-ento-020117-043145>.
- Hoback, W.W., Stanley, D.W., 2001. Insects in hypoxia. *J. Insect Physiol.* 47, 533–542. [https://doi.org/10.1016/S0022-1910\(00\)00153-0](https://doi.org/10.1016/S0022-1910(00)00153-0).
- Hutchins, E.J., Bronner, M.E., 2021. A spectrum of cell states during the epithelial-to-mesenchymal transition. *Methods Mol. Biol.* 2179, 3–6. https://doi.org/10.1007/978-1-0716-0779-4_1.
- Ikeda, K., Kawakami, K., 1995. DNA binding through distinct domains of zinc-finger-homeodomain protein AREB6 has different effects on gene transcription. *Eur. J. Biochem.* 233, 73–82. <https://doi.org/10.1111/j.1432-1033.1995.073.1.x>.
- Jackai, L.E.N., Daoust, R.A., 1986. Insect pests of cowpeas. *Annu. Rev. Entomol.* 31, 95–119. <https://doi.org/10.1146/annurev.en.31.010186.000523>.
- Kharel, K., Mason, L.J., Murdock, L.L., Baributsa, D., 2019. Efficacy of hypoxia against *Tribolium castaneum* (Coleoptera: Tenebrionidae) throughout ontogeny. *J. Econ. Entomol.* 112, 1463–1468. <https://doi.org/10.1093/jee/toz019>.
- Lai, Z.C., Fortini, M.E., Rubin, G.M., 1991. The embryonic expression patterns of *zfh-1* and *zfh-2*, two *Drosophila* genes encoding novel zinc-finger homeodomain proteins. *Mech. Dev.* 34, 123–134. [https://doi.org/10.1016/0925-4773\(91\)90049-c](https://doi.org/10.1016/0925-4773(91)90049-c).
- Lait, J.H., Dyson, H.J., Wright, P.E., 2000. DNA-induced alpha-helix capping in conserved linker sequences is a determinant of binding affinity in Cys₂-His₂ zinc fingers. *J. Mol. Biol.* 295, 719–727. <https://doi.org/10.1006/jmbi.1999.3406>.
- Langmead, B., Trapnell, C., Pop, M., Salzberg, S.L., 2009. Ultrafast and memory-efficient alignment of short DNA sequences to the human genome. *Genome Biol.* 10, R25. <https://doi.org/10.1186/gb-2009-10-3-r25>.
- Lee, B., Barretto, E.C., Grewal, S.S., 2019. TORC1 modulation in adipose tissue is required for organismal adaptation to hypoxia in *Drosophila*. *Nat. Commun.* 10, 1878. <https://doi.org/10.1038/s41467-019-09643-7>.
- Lee, S.J., Feldman, R., O'Farrell, P.H., 2008. An RNA interference screen identifies a novel regulator of target of rapamycin that mediates hypoxia suppression of translation in *Drosophila* S2 cells. *Mol. Biol. Cell* 19, 4051–4061. <https://doi.org/10.1091/mbc.E08-03-0265>.
- Lehmann, W., Mossmann, D., Kleemann, J., Mock, K., Meisinger, C., Brummer, T., Herr, R., Brabletz, S., Stemmler, M.P., Brabletz, T., 2016. ZEB1 turns into a transcriptional activator by interacting with YAP1 in aggressive cancer types. *Nat. Commun.* 7, 10498. <https://doi.org/10.1038/ncomms10498>.
- Li, H., Zou, J., Yu, X.H., Ou, X., Tang, C.K., 2021. Zinc finger E-box binding homeobox 1 and atherosclerosis: new insights and therapeutic potential. *J. Cell. Physiol.* 236, 4216–4230. <https://doi.org/10.1002/jcp.30177>.
- Li, Y., Padmanabha, D., Gentile, L.B., Dumur, C.I., Beckstead, R.B., Baker, K.D., 2013. HIF- and non-HIF-regulated hypoxia responses require the estrogen-related receptor in *Drosophila melanogaster*. *PLoS Genet.* 9, e1003230. <https://doi.org/10.1371/journal.pgen.1003230>.
- Love, M.I., Huber, W., Anders, S., 2014. Moderated estimation of fold change and dispersion for RNA-seq data with DESeq2. *Genome Biol.* 15, 550. <https://doi.org/10.1186/s13059-014-0550-8>.
- Mahneva, O., Caplan, S.L., Ivko, P., Dawson-Scully, K., Milton, S.L., 2019. NO/cGMP/PKG activation protects *Drosophila* cells subjected to hypoxic stress. *Comp. Biochem. Physiol. C Toxicol. Pharmacol.* 223, 106–114. <https://doi.org/10.1016/j.cbpc.2019.05.013>.
- Marceau, A.H., Felthousen, J.G., Goetsch, P.D., Iness, A.N., Lee, H.W., Tripathi, S.M., Strome, S., Litovchick, L., Rubin, S.M., 2016. Structural basis for LIN54 recognition of CHR elements in cell cycle-regulated promoters. *Nat. Commun.* 7, 12301. <https://doi.org/10.1038/ncomms12301>.
- Myllymaki, H., Ramet, M., 2013. Transcription factor *zfh1* downregulates *Drosophila* Imd pathway. *Dev. Comp. Immunol.* 39, 188–197. <https://doi.org/10.1016/j.dci.2012.10.007>.
- Nishimura, G., Manabe, I., Tsushima, K., Fujii, K., Oishi, Y., Imai, Y., Maemura, K., Miyagishi, M., Higashi, Y., Kondoh, H., Nagai, R., 2006. δ EF1 mediates TGF- β signaling in vascular smooth muscle cell differentiation. *Dev. Cell* 11, 93–104. <https://doi.org/10.1016/j.devcel.2006.05.011>.
- Ongwijitwat, S., Wong-Riley, M.T., 2005. Is nuclear respiratory factor 2 a master transcriptional coordinator for all ten nuclear-encoded cytochrome c oxidase subunits in neurons? *Gene* 360, 65–77. <https://doi.org/10.1016/j.gene.2005.06.015>.
- Postigo, A.A., Dean, D.C., 1999. ZEB represses transcription through interaction with the corepressor CtBP. *Proc. Natl. Acad. Sci. U. S. A.* 96, 6683–6688. <https://doi.org/10.1073/pnas.96.12.6683>.
- Postigo, A.A., Depp, J.L., Taylor, J.J., Kroll, K.L., 2003. Regulation of Smad signaling through a differential recruitment of coactivators and corepressors by ZEB proteins. *EMBO J.* 22, 2453–2462. <https://doi.org/10.1093/emboj/cdg226>.
- Postigo, A.A., Ward, E., Skeath, J.B., Dean, D.C., 1999. *zfh-1*, the *Drosophila* homologue of ZEB, is a transcriptional repressor that regulates somatic myogenesis. *Mol. Cell Biol.* 19, 7255–7263. <https://doi.org/10.1128/mcb.19.10.7255>.
- Quandt, K., Frech, K., Karas, H., Wingender, E., Werner, T., 1995. MatInd and MatInspector: new fast and versatile tools for detection of consensus matches in nucleotide sequence data. *Nucleic Acids Res.* 23, 4878–4884. <https://doi.org/10.1093/nar/23.23.4878>.
- Reiling, J.H., Hafen, E., 2004. The hypoxia-induced paralogs Scylla and Charybdis inhibit growth by down-regulating S6K activity upstream of TSC in *Drosophila*. *Genes Dev.* 18, 2879–2892. <https://doi.org/10.1101/gad.322704>.
- Roberts, A., Pachter, L., 2013. Streaming fragment assignment for real-time analysis of sequencing experiments. *Nat. Methods* 10, 71–73. <https://doi.org/10.1038/nmeth.2251>.
- Sadasivam, S., Duan, S., DeCaprio, J.A., 2012. The MuvB complex sequentially recruits B-Myb and FoxM1 to promote mitotic gene expression. *Genes Dev.* 26, 474–489. <https://doi.org/10.1101/gad.181933.111>.
- Sayadi, A., Martinez Barrio, A., Immonen, E., Dainat, J., Berger, D., Tellgren-Roth, C., Nystedt, B., Arnqvist, G., 2019. The genomic footprint of sexual conflict. *Nat. Ecol. Evol.* 3, 1725–1730. <https://doi.org/10.1038/s41559-019-1041-9>.
- Scott, M.P., Tamkun, J.W., Hartzell 3rd, G.W., 1989. The structure and function of the homeodomain. *Biochim. Biophys. Acta* 989, 25–48. [https://doi.org/10.1016/0304-419x\(89\)90033-4](https://doi.org/10.1016/0304-419x(89)90033-4).
- Sekido, R., Murai, K., Kamachi, Y., Kondoh, H., 1997. Two mechanisms in the action of repressor δ EF1: binding site competition with an activator and active repression. *Gene Cell.* 2, 771–783. <https://doi.org/10.1046/j.1365-2443.1997.1570355.x>.
- Shoshani, T., Faerman, A., Mett, I., Zelin, E., Tenne, T., Gorodin, S., Moshel, Y., Elbaz, S., Budanov, A., Chajut, A., Kalinski, H., Kamer, I., Rozen, A., Mor, O., Keshet, E., Leshkowitz, D., Einat, P., Skaliter, R., Feinstein, E., 2002. Identification of a novel hypoxia-inducible factor 1-responsive gene, RTP801, involved in apoptosis. *Mol. Cell Biol.* 22, 2283–2293. <https://doi.org/10.1128/mcb.22.7.2283-2293.2002>.
- Silva, M.G.C., Silva, G.N., Sousa, A.H., Freitas, R.S., Silva, M.S.G., Abreu, A.O., 2018. Hermetic storage as an alternative for controlling *Callosobruchus maculatus* (Coleoptera: Chrysomelidae) and preserving the quality of cowpeas. *J. Stored Prod. Res.* 78, 27–31. <https://doi.org/10.1016/j.jspr.2018.05.010>.
- Tasaki, R., Matsuura, K., Iuchi, Y., 2018. Hypoxia adaptation in termites: hypoxic conditions enhance survival and reproductive activity in royals. *Insect Mol. Biol.* 27, 808–814. <https://doi.org/10.1111/imb.12519>.
- Van der Geest, H.G., 2007. Behavioural responses of caddisfly larvae (*Hydropsyche angustipennis*) to hypoxia. *Contrib. Zool.* 76, 255–260. <https://doi.org/10.1163/18759866-07604004>.
- Van Voorhies, W.A., 2009. Metabolic function in *Drosophila melanogaster* in response to hypoxia and pure oxygen. *J. Exp. Biol.* 212, 3132–3141. <https://doi.org/10.1242/jeb.031179>.
- VandenBrooks, J.M., Gstrein, G., Harmon, J., Friedman, J., Olsen, M., Ward, A., Parker, G., 2018. Supply and demand: how does variation in atmospheric oxygen during development affect insect tracheal and mitochondrial networks? *J. Insect Physiol.* 106, 217–223. <https://doi.org/10.1016/j.jinsphys.2017.11.001>.
- Vigne, P., Frelin, C., 2010. Hypoxia modifies the feeding preferences of *Drosophila*. Consequences for diet dependent hypoxic survival. *BMC Physiol.* 10, 8. <https://doi.org/10.1186/1472-6793-10-8>.
- Wang, L., Cheng, W., Meng, J., Speakmon, M., Qiu, J., Pillai, S., Zhu-Salzman, K., 2019. Hypoxic environment protects cowpea bruchid (*Callosobruchus maculatus*) from electron beam irradiation damage. *Pest Manag. Sci.* 75, 726–735. <https://doi.org/10.1002/ps.5172>.
- Werner, T., Fessele, S., Maier, H., Nelson, P.J., 2003. Computer modeling of promoter organization as a tool to study transcriptional coregulation. *Faseb. J.* 17, 1228–1237. <https://doi.org/10.1096/fj.02-0955rev>.
- Wingrove, J.A., O'Farrell, P.H., 1999. Nitric oxide contributes to behavioral, cellular, and developmental responses to low oxygen in *Drosophila*. *Cell* 98, 105–114. [https://doi.org/10.1016/S0092-8674\(00\)80610-8](https://doi.org/10.1016/S0092-8674(00)80610-8).
- Ye, J., Fang, L., Zheng, H., Zhang, Y., Chen, J., Zhang, Z., Wang, J., Li, S., Li, R., Bolund, L., Wang, J., 2006. WEGO: a web tool for plotting GO annotations. *Nucleic Acids Res.* 34, W293–W297. <https://doi.org/10.1093/nar/gkl031>.
- Ye, J., Zhang, Y., Cui, H., Liu, J., Wu, Y., Cheng, Y., Xu, H., Huang, X., Li, S., Zhou, A., Zhang, X., Bolund, L., Chen, Q., Wang, J., Yang, H., Fang, L., Shi, C., 2018. WEGO 2.0: a web tool for analyzing and plotting GO annotations, 2018 update. *Nucleic Acids Res.* 46, W71–W75. <https://doi.org/10.1093/nar/gky400>.
- Yu, C.P., Chen, S.C., Chang, Y.M., Liu, W.Y., Lin, H.H., Lin, J.J., Chen, H.J., Lu, Y.J., Wu, Y.H., Lu, M.Y., Lu, C.H., Shih, A.C., Ku, M.S., Shiu, S.H., Wu, S.H., Li, W.H., 2015. Transcriptome dynamics of developing maize leaves and genome-wide prediction of cis elements and their cognate transcription factors. *Proc. Natl. Acad. Sci. U. S. A.* 112, E2477–E2486. <https://doi.org/10.1073/pnas.1500605112>.
- Zhang, Z., Yin, C., Liu, Y., Jie, W., Lei, W., Li, F., 2014. iPathCons and iPathDB: an improved insect pathway construction tool and the database. *Database* 1–11. <https://doi.org/10.1093/database/bau105>, 2014.
- Zhao, D., Zhang, Z., Cease, A., Harrison, J., Kang, L., 2013. Efficient utilization of aerobic metabolism helps Tibetan locusts conquer hypoxia. *BMC Genom.* 14, 631. <https://doi.org/10.1186/1471-2164-14-631>.
- Zhao, D.J., Zhang, Z.Y., Harrison, J., Kang, L., 2012. Genome-wide analysis of transcriptional changes in the thoracic muscle of the migratory locust, *Locusta migratoria*, exposed to hypobaric hypoxia. *J. Insect Physiol.* 58, 1424–1431. <https://doi.org/10.1016/j.jinsphys.2012.08.006>.
- Zhou, D., Xue, J., Lai, J.C., Schork, N.J., White, K.P., Haddad, G.G., 2008. Mechanisms underlying hypoxia tolerance in *Drosophila melanogaster*: hairy as a metabolic switch. *PLoS Genet.* 4, e1000221. <https://doi.org/10.1371/journal.pgen.1000221>.